PAUL SCHERRER INSTITUT	SLS 2.0
Vertical beam size minimization in the SLS booster	Document identification SLS2-KJ81-001-1
Author(s) J. Kallestrup	February 18, 2021

1 Introduction

A strong motivation for the minimization of the vertical beam size is the usage of the emittance exchange by coupling resonance crossing technique for the horizontal off-axis injection into the SLS 2.0 storage ring. Using this technique, the horizontal and vertical emittances are exchanged in the booster synchrotron shortly before the extraction of the beam. This leads to a small horizontal beam size at the injection into the storage ring, leading to a reduction of the needed acceptance for capturing the injection beam [1]. If a smaller vertical emittance can be achieved, then a smaller horizontal emittance can be achieved after the coupling resonance crossing.

The vertical beam size arises from transverse coupling and spurious dispersion. The transverse coupling leads to a vertical emittance increase through betatron coupling (the sharing of horizontal emittance into the vertical plane when $Q_x - Q_y \approx 0$) but also the coupling of horizontal dispersion into the vertical plane, generating vertical emittance without decrease of the horizontal emittance.

During initial commissioning, the orbit was corrected for good injection into the booster. Due to the limited strength of the corrector magnets it was not possible to ramp the same corrector pattern to 2.4 GeV. Therefore, no ramping of the correctors was done and subsequently there was no orbit correction at the extraction energy. Nevertheless, the booster has worked more or less faultlessly for 20 years. The uncorrected vertical orbit however has the drawback that a vertical orbit offset in sextupole magnets leads to a skew quadrupole component, contributing to the transverse coupling of the machine. All dipoles in the booster contains sextupole components from chromaticity correction. In [1] the amplitude of the coupling coefficient was measured to be $|C| \approx 0.02$, a relatively large value, expected to stem from the vertical orbit offsets in magnets with sextupole gradients.

Only ≈ 5 beam position monitors were available in the booster, and therefore the vertical orbit cannot readily be corrected. Instead, it was realized that a direct minimization of the vertical beam size, measured on the ABRDI-SM-2 screen monitor in the booster-to-ring transfer line, would most likely lead to the desired result. The ABRDI-SM-2 screen monitor was chosen instead of ABRDI-SM-3 due to the high vertical beta function of $\approx 40\,\mathrm{m}$.

2 Vertical beam size minimization

The minimization of the vertical beam size consists of two steps of scanning corrector magnets: a) closed-orbit bumps using three correctors and b) single-corrector minimization. The beam size was only evaluated at the nominal extraction time. A linear ramp of the corrector was used due to simplicity.

For the closed-orbit step, each possible combination of three subsequent vertical corrector was used closed orbit bumps. For each combination, the bump amplitude was first increased; if the bump increase lead to a smaller vertical beam size, the bump amplitude would be further increased. If a increase did not work, a decrease was tried until no further improvement of the vertical beam size was found. Due to having 54 different closed orbit combinations, only 5 samples was used for each setting to evaluate the beam size. This is deemed acceptable, because the whole cycle of 54 correctors was iterated 3 times with decreasing step size.

Since closed-orbit bumps are often limited in amplitude, we continued with a similar minimization procedure simply stepping up/down each corrector individually. This often lead to a small improvement in the vertical beam size. The results of one minimization campaign is given on Fig. 1. The dispersion was measured on both ABRDI-SM-2 and ABRDI-SM-3 - results of vertical dispersion before and after the minimization is plotted in Fig. 2. The minimization almost completely suppresses the vertical dispersion on the monitors. Horizontal dispersion is virtually unchanged. Finally, we measured the coupling coefficient, |C|, for different scalings of the corrector pattern. Fig. 3 shows a few examples of closest tune approach spectra found using scaling of the applied corrector pattern. 0% means that the correct pattern is not applied at all, why 100% means that the full strength of the minimizing pattern is used. The coupling coefficient is expected to linearly depend on the corrector pattern through the equation

$$C = -\frac{1}{2\pi} \oint ds \ 2k_2 y(s) \sqrt{\beta_x(s)\beta_y(s)} e^{-i\left[\phi_x(s) - \phi_y(s) + \frac{s}{R}\Delta\right]},\tag{1}$$

where y(s) is the vertical orbit off-set in the sextupole of strength k_2 . This linear dependency is indeed found in Fig. 4, where we have plotted the found values of |C| as a function of the corrector pattern scaling. We find from the linear fit that by using the full corrector pattern we have a coupling coefficient of $|C| \approx 0.002$. This is a factor 10 decrease with respect to the previous normal operation of the booster.

Note that the value for |C| at 0% scaling in Fig. 2 is much larger (≈ 0.035) than the value reported in [1] (≈ 0.020). This is because the chromaticity was corrected after the initial paper by almost doubling the SD sextupole family current to fight the fast head-tail instability, see [3]. This lead to a significant increase in the coupling of the machine. Fig. 3 is however made using data prior to the chromaticity correction.

After performing the vertical beam size minimization, the crossing of the linear coupling resonance to achieve emittance exchange must be re-established due to the smaller coupling of the machine. A very small coupling can lead to a non-adiabatic emittance exchange - See [2] for details on the implemented emittance exchange and the consequences of small coupling.

References

- [1] J. Kallestrup and M. Aiba, "Emittance exchange in electron booster synchrotron by coupling resonance crossing", Phys. Rev. Accel. Beams 23, 020701 (2020)
- [2] J. Kallestrup, "Emittance exchange by coupling resonance crossing in the SLS booster synchrotron", SLS note: SLS2-KJ81-003
- [3] J. Kallestrup, "SLS booster fast head-tail instability characterization and cure", SLS note: SLS2-KJ81-002

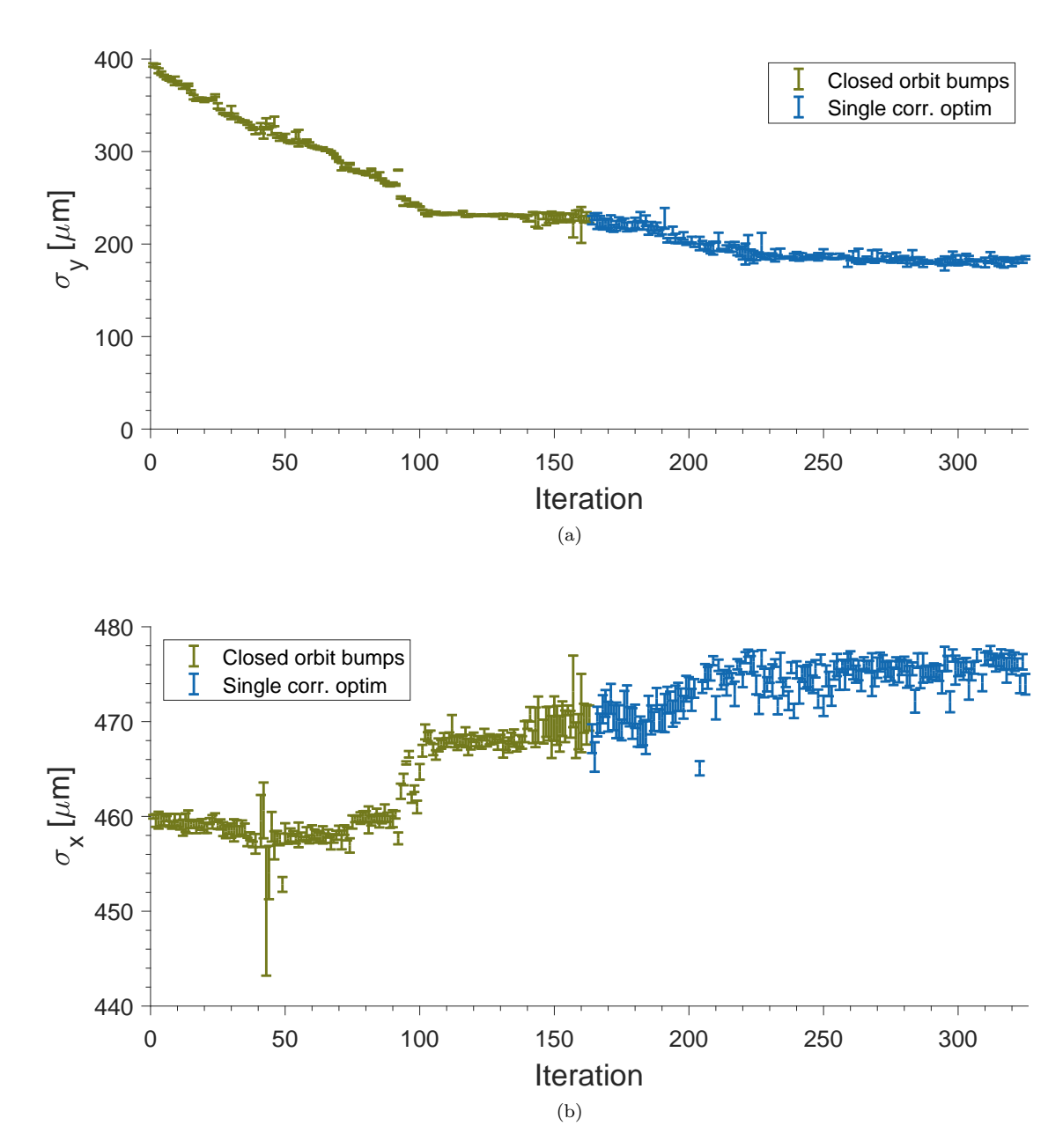


Figure 1: a) Iterative decrease of vertical beam size on ABRDI-SM-2 screen monitor using first a closed-orbit bump based optimization followed by a single-corrector optimization of the SLS Booster correctors.

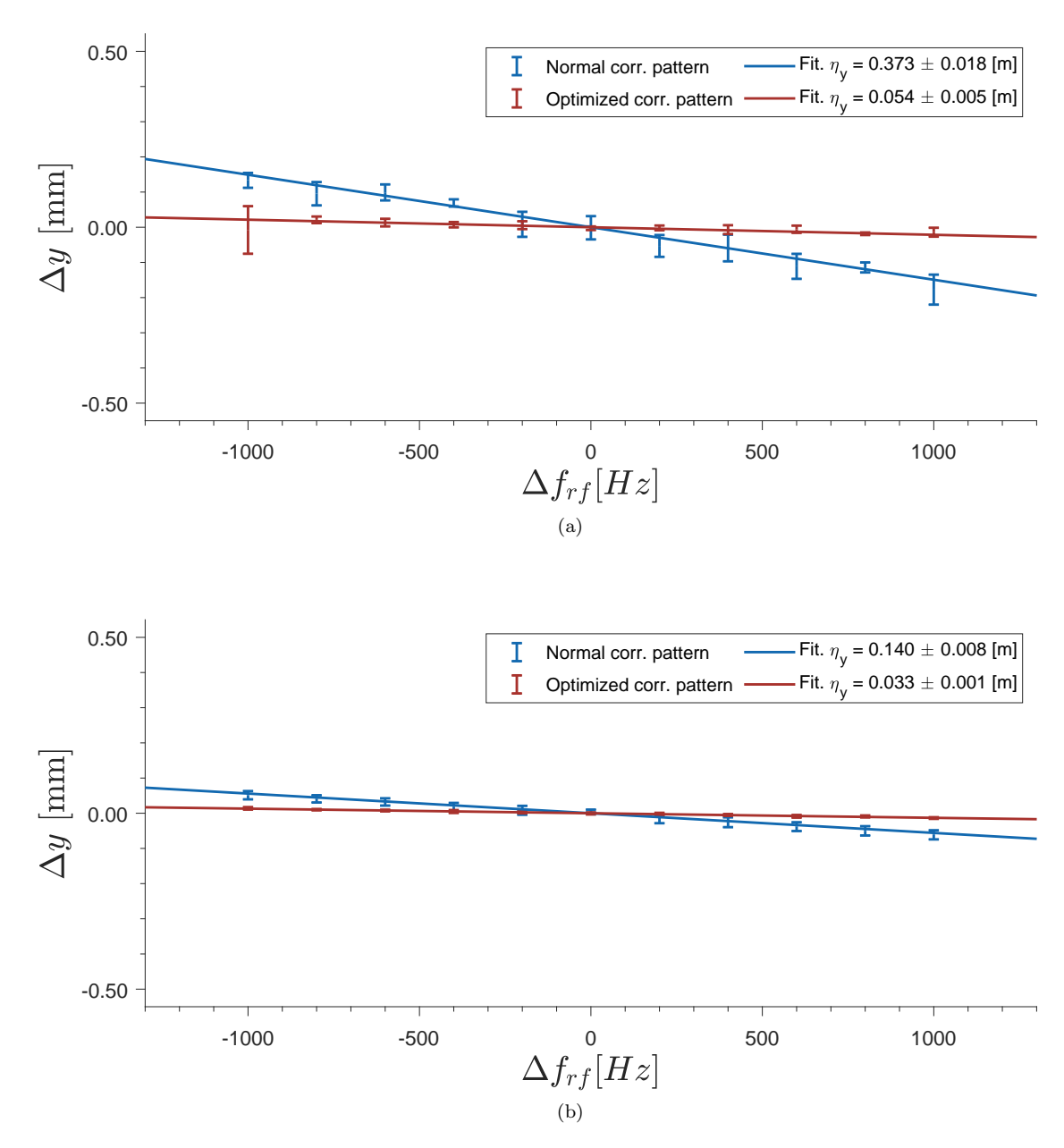


Figure 2: Vertical dispersion measurements on the ABRDI-SM-2 (top) and ABRDI-SM-3 (bottom) screen monitors in the SLS Booster-to-Ring Transfer Line with and without a corrector pattern leading to a minimization of the vertical beam size.

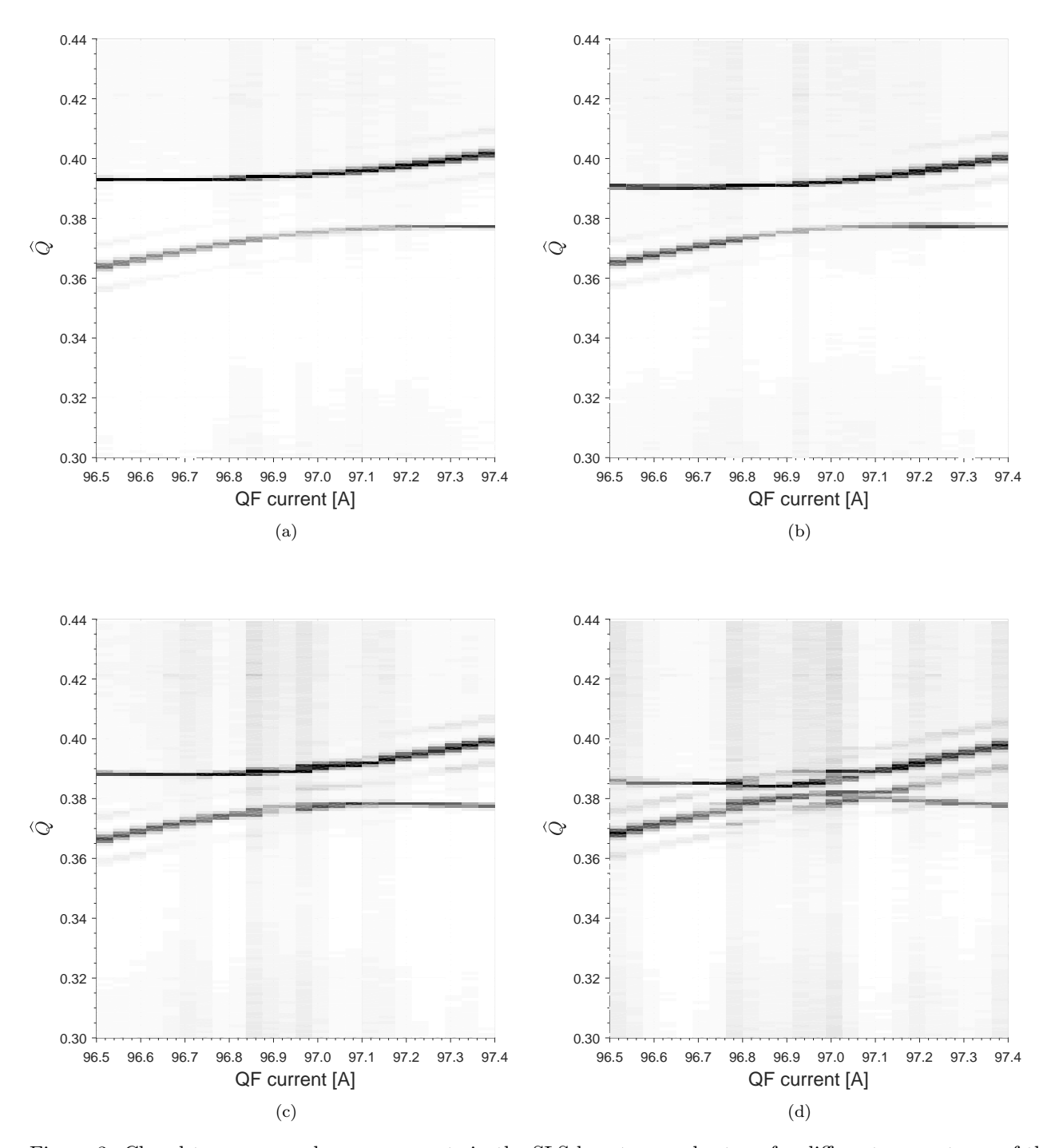


Figure 3: Closed tune approach measurements in the SLS booster synchrotron for different percentages of the corrector pattern leading to a minimized vertical beam size. a) 0%, b) 20%, c) 40% and d) 80%.

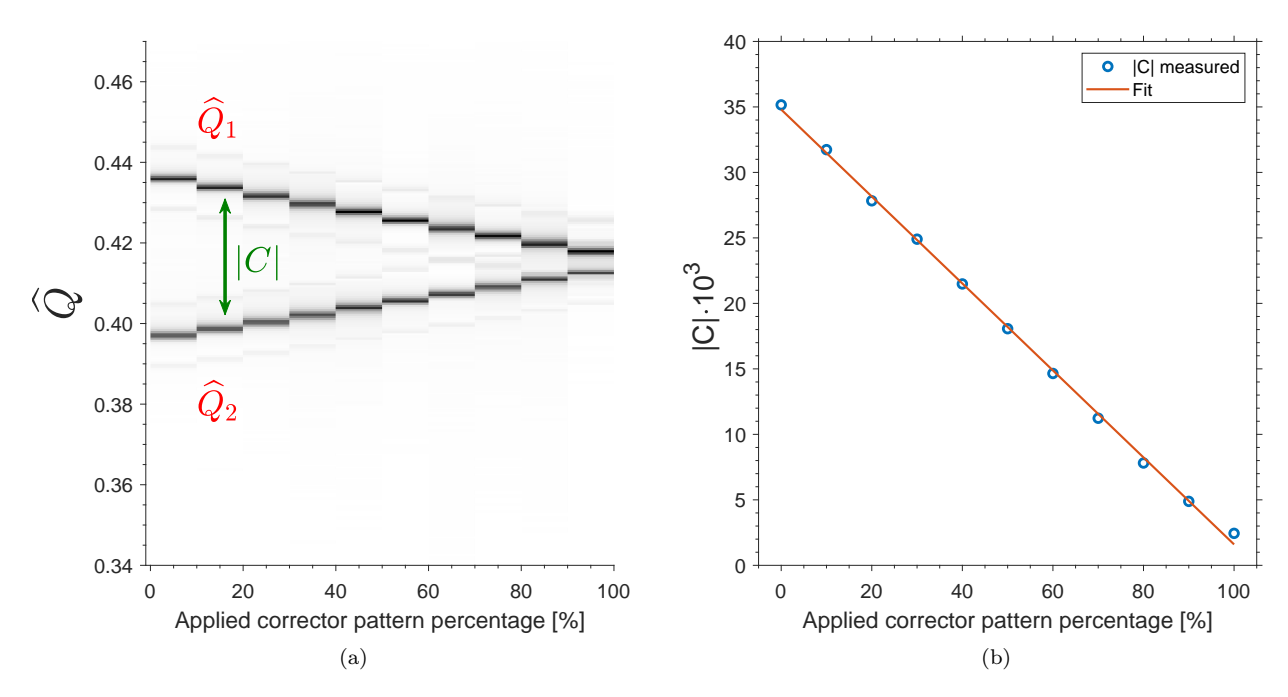


Figure 4: Coupling coefficient as a function of the applied corrector pattern percentage.